IEEE Access
Multidisciplinary : Rapid Review : Open Access Journal

Received May 13, 2019, accepted June 26, 2019, date of publication July 9, 2019, date of current version July 31, 2019.

Digital Object Identifier 10.1109/ACCESS.2019.2927632

Improving Performance of Retaining Walls Under Dynamic Conditions Developing an Optimized ANN Based on Ant Colony Optimization Technique

CHUANHUA XU[1], BEHROUZ GORDAN[2], MOHAMMADREZA KOOPIALIPOOR[3], DANIAL JAHED ARMAGHANI[4], M. M. TAHIR[5], AND XILIANG ZHANG[1]

[1]State Key Laboratory of Safety and Health for Metal Mines, Sinosteel Maanshan Institute of Mining Research, Company, Ltd., Ma'anshan 243000, China
[2]Department of Geotechnics and Transportation, Faculty of Civil Engineering, Universiti Teknologi Malaysia, Skudai 81310, Malaysia
[3]Faculty of Civil and Environmental Engineering, Amirkabir University of Technology, Tehran 15914, Iran
[4]Institute of Research and Development, Duy Tan University, Da Nang 550000, Vietnam
[5]UTM Construction Research Centre, Institute for Smart Infrastructure and Innovative Construction (ISIIC), School of Civil Engineering, Faculty of Engineering, Universiti Teknologi Malaysia, Johor Bahru 81310, Malaysia

Corresponding author: Danial Jahed Armaghani (danialarmaghani@gmail.com)

ABSTRACT In this paper, a combination of artificial neural network and ant colony optimization (ANN-ACO) was used for dynamic conditions of retaining wall structures. The retaining walls produce different responses to dynamic loads. The applied data of this study comprising of wall height and thickness, soil density, internal friction angle, and stone density. The walls were designed in a variety of dynamic conditions. Various conditions were considered for the design of the retaining wall structures. Then, an extended data set was created for the next step. After that, the new systems were implemented using optimized artificial intelligence techniques. The neural network provided strong relationships between various wall parameters. The design of various networks in the present research led to the best evaluation of the dynamic conditions of the retaining walls. Under these conditions, an ACO was used for optimal design. Effects of parameters varied due to different wall conditions when dynamic loads were considered. Therefore, the impact of parameters was evaluated using hybrid ANN-ACO to increase the efficiency. These designs provided more control over dangers by dynamic loads of a retaining wall structure.

INDEX TERMS ACO, ANN, optimization, prediction, retaining wall, safety factor.

I. INTRODUCTION

Since the original study of Mononobe [1] and analytical study of Okabe [2], there have been several experimental, analytical and numerical studies of the dynamic behavior of retaining walls (RWs) due to offer a method for rational modeling. The various methodologies were applied to investigate active earth pressures can be alienated into three main methods such as analytical, numerical, and experimental. Based on previous investigations, a recent alternative to the Mononobe-Okabe (M-O) method for plastic soils was presented by Mylonakis *et al.* [3]. They offered a closed-form stress plasticity solution for gravitational and earthquake-induced earth pressures on RWs. Moreover, Nakumara [4] and Al-Atik and Sitar [5] recently carried out separate shake table tests using centrifuge facilities, and both separately concluded that the measured earth pressure during shaking was lower than the M-O method predictions. Nakamura [4] also highlighted that the inertial force was not always transmitted to the wall and backfill simultaneously. Dewoolkar *et al.* [6] carried out centrifuge dynamic excitation tests with fixed-base cantilever walls supporting saturated, liquefiable, cohesion less backfills. Based on the results, Dewoolkar *et al.* [6] found that excess pore pressure generation is increased significantly to seismic lateral earth pressure in the saturated backfill. They also pointed out that the maximum dynamic thrust is proportional to the input base acceleration. Green and Ebeling [7] designed the dynamically induced

The associate editor coordinating the review of this manuscript and approving it for publication was Haruna Chiroma.

lateral earth pressure on the stem portion of a concrete cantilever earth RW with dry medium dense sand using finite difference code FLAC. They determined that at very low level of seismic activity, the seismic earth pressures are in agreement with M-O predictions; however, as accelerations increased, seismic earth pressures are larger than those forecasted by the M-O method. Gazetas *et al.* [8] completed models of L-shaped walls, pre-stressed anchored pile walls, and reinforced soil walls, employing both linear and non-linear soil models. Using those models, Gazetas *et al.* [8] considered some parameters such as the wall flexibility, foundation soil deformability, material soil yielding and soil wall separation and sliding tends to reduce the effects of dynamic excitations on those walls. They also used an FE model to simulate a case history in which a RW performed well during an actual earthquake. Psarropoulos *et al.* [9] implemented a study to confirm the assumptions of Veletsos and Younan analytical solution and to propose the range if its applicability. The numerical designs were presented using the commercial finite-element method (FEM). The versatility of the numerical methods, finite-element and finite-difference, permitted the treatment of more realistic situations that are not amenable to analytical solution including the heterogeneity of the retained soil, and translational flexibility of the wall foundation. To investigate the characteristics of the lateral seismic soil pressure on building walls, Ostadan [10] performed a series of soil-structure-interaction analyses using SASSI. Using the concept of a single degree-of-freedom, Ostadan [10] proposed a simplified method to predict maximum seismic soil pressures for building walls resting on firm foundation material. The method resulted in dynamic earth pressure profiles comparable to or larger than the Wood [11] solution, with the maximum earth pressure occurring at the top of the wall.

Using intelligent models in engineering problems can improve the performance of structures. Ant colony optimization (ACO) is a one of the most interesting optimization techniques which belonging to the group of swarm intelligence algorithm and aims to find an optimal path (best solution) within a computational space. Inspired by the exploratory behavior or life of ants in search of food, the way copies the behavior of ants in finding a path between their congestion and the source of food [12], [13]. The first algorithm of ACO was introduced as an innovative method for finding complex optimization problems in early 1990s [13]. Subsequently, various algorithms were introduced as the ant colony system [12] and the maximum/minimum ant system [44]. Later, ACO was developed to solve multi-objective optimization problems. The multi-objective ACO consists of an ACO algorithm as a basis as well as specific algorithm components for overcoming the multi-objective optimization. This can be done by a variety of ways such as the use of various pheromone matrices for any purpose, or the use of multi-colony approach with a colony for each case [14], [15]. ACO is also accepted to be applied for continuous optimization problems.

In this research, a combination of two models of artificial neural network (ANN) and ACO was presented for the dynamic conditions of RWs. Various conditions are considered for the design of the RW. Then, an extended data set was created for the next step. In the intelligent section, different models were developed to obtain an appropriate relationship for SF determination. After that, a new methodology based on ACO was used to optimize design engineering. The ANN models were controlled by ACO to improve various conditions with different safety factor (SF). Using this combination, a wide range of issues can be implemented and designed.

II. MATERIAL AND METHODS

A. ARTIFICIAL NEURAL NETWORK

Since the 1940s, ANNs have been used as a predictive tool in fields of science and engineering [16]–[18]. ANNs are flexible mathematical structures that can define a high-level and non-linear relationship between input and output parameters without solving complex partial differential equations (PDEs) [13], [15], [19]. ANNs are based on a hypothesis similar to the neural structure and human learning process. They have been successfully used to build environmental controls. These networks are made of three main components including layers (input, hidden and output), neurons, and weights among neurons. Each layer is made of neurons. In particular, the output layer neurons produce results of network computations. Weights indicate the effect factor of neurons. A training process is usually necessary to make optimal computations to determine weights prior to the practical application in system controls [20]. In the ANN training process, a weight is assigned to all links, and then, all weighted inputs are combined and the output neuron is generated. The following equation is used:

$$y_t = \alpha_0 + \sum_{j=1}^{n} \alpha_j f(\sum_{i=1}^{m} \beta_{ij} y_{t-1} + \beta_{0j}), \quad [\mathrm{i} = 1, \ldots, \mathrm{m} \text{ and } \mathrm{j} = 1, \ldots, \mathrm{n}] \tag{1}$$

where m is the number of input nodes; n is the number of hidden nodes; α_j represents the vector of weights from hidden to output nodes; and β_{ij} represents weights from input to hidden nodes. α_0 and β_{0j} are weights of arches resulting from biased terms that always have values equal to 1; and f is the transfer function. Figure 1 shows the connection structure of the input data, weights, constant coefficients, activation functions and output.

B. ANT COLONY OPTIMIZATION

The ACO is a meta-heuristic optimization algorithm inspired by the search behavior of ants to identify the shortest path from their nest to a food source using pheromone traces [21]. In this algorithm, the decision space in the optimization problem is represented by a graph where nodes and sides are as decision variables and decision variable options, respectively. The solution is made by ant passing on the graph and selecting a side on each node. As the ants go forward the graph, they left behind pheromones. The highly used paths have

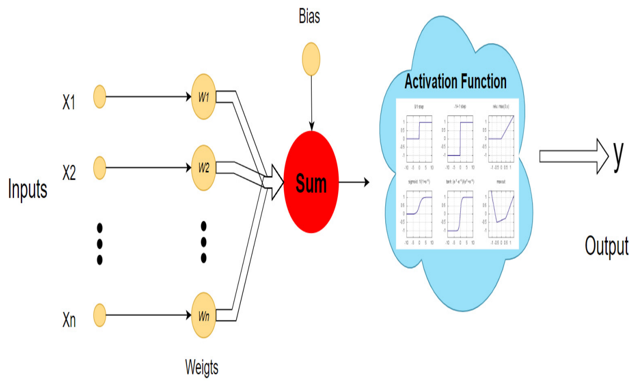

FIGURE 1. A structure of ANN modeling.

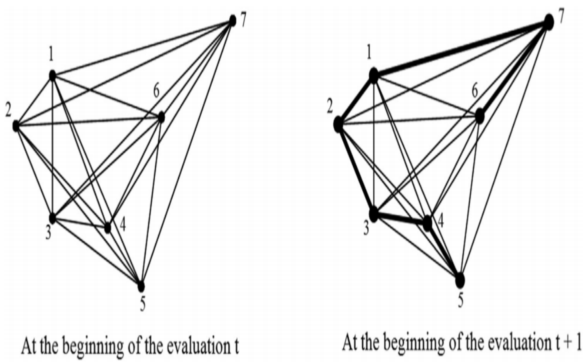

FIGURE 2. An sample of the pheromone performance for a seven-city TSP [23].

higher concentrations of pheromones and are more likely to be selected by other ants in the future [22]. Figure 2 shows an example of the pheromone distribution for the traveling salesman problem (TSP) with seven cities. In this figure, thicker sides (5-4-3-2-1-6-7) in the right diagram have higher pheromones in proportional to levels. In each ACO process repeat, all members of a colony traverse the graph; and each one produces a response. After each repeat, the paths leading to better overall responses receive more pheromones as rewards, thereby increasing the chance of their selection in subsequent repeats. Therefore, better responses evolve due to the increased number of repeats. At each decision point, the probability that an ant selects a certain side (e.g. AB side) can be determined using the following equation:

$$P_{AB} = \frac{[\tau_{AB}(t)]^{\alpha}[\eta_{AB}]^{\beta}}{\sum_{B=1}^{N_A}[\tau_{AB}(t)]^{\alpha}[\eta_{AB}]^{\beta}} \tag{2}$$

where, t is the repeat index; *AB(t)* is the size of Pheromone side (*AB*) in the repeat t; and *AB* is the visibility of side (*AB*) leading to the provision of a biased amount of local optimal solutions at the desired decision point; *NA* is the set of all decision options at the decision point A; α is the importance of pheromone; and β is the coefficient of the visibility importance. Updating pheromones on each side (e.g. *AB* side) after

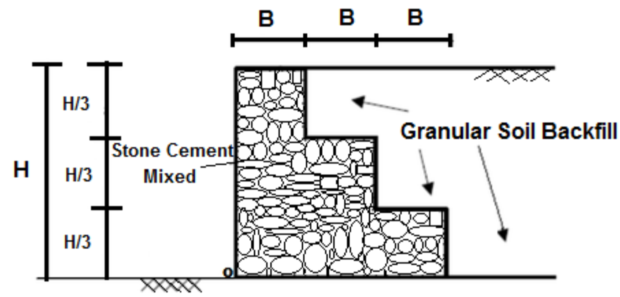

FIGURE 3. Dimension model for gravity masonry retaining wall.

each repeat can be obtained by the following equation [21]:

$$\tau_{AB}(t+1) = \rho\tau_{AB}(t) + \Delta\tau_{AB}(t) \tag{3}$$

where, ρ is the durability factor of pheromone indicating the evaporation rate of pheromone from one repeat to another; $\tau_{AB}(t)$ is the amount of added pheromone to the side (*AB*) in the repeat t and it can be obtained using different approaches such as ant colony system, elite ant system, rank-based ant system, and MAX-MIN ant system [23]. ACO repeats continue as long as the specific stop criterion is fulfilled such as completing a certain number of iteration or when there is no improvement in the objective function.

C. DATA COLLECTION

To create a dataset, different designs were performed based on several parameters, and finally the amount of SF was determined for model. The process consisted of model dimensions, material properties, introducing boundary conditions, and seismic motion. Mononobe's method utilizing visual basic language was applied to obtain SF values in this study. Several homogenous soils such as sand, gravel-sand and gravel behind the retaining masonry wall (in terms of material, $\gamma = 17, 17.50, 18, 18.5$ and 19 ton/m^3) with different modes were designed to achieve SF. RWs with heights of 3, 4, 5, 6, 7, 8, 9 and 10 m, were modeled. The location of models were assumed on the bedrock because of its rigid behavior. In addition, the wall width of 0.5, 0.6, 0.7 and 0.8 m were assumed for all models. Moreover, the range of gravity for stone mixed cement was considered as 20, 24 and 28 ton/m^3. Figure 3 shows the details of RW model considered in this study. It can be seen that, both angles β and i are zero in this study. The Mohr–Coulomb failure criterion was considered for the models. The values of cohesions were assumed as 0 for granular soil and internal friction angles of 30°, 35°, 40°, and 45° were applied in the analyses process. Granular soil was used because of avoiding the pure water pressure behind the walls. It can be noted that, the earthquake motion effect is an important role to control the RWs behavior. Figure 4 shows the distribution of active pressure for static and dynamic conditions and body forces for soil and stone blocks. As mentioned by Kramer 1996, peak ground acceleration (PGA) is an important measure of earthquake acceleration on the ground. In the current research, the amplitudes of PGA were assumed

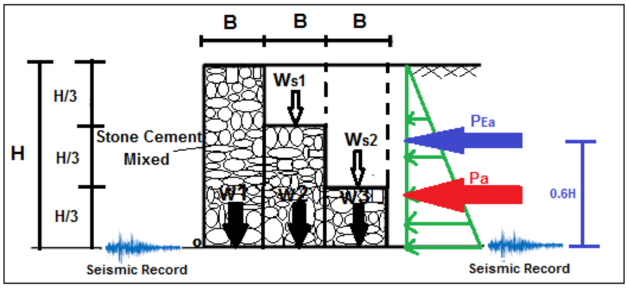

FIGURE 4. Distribution of active force for static and dynamic conditions with body forces for soil and Stone blocks.

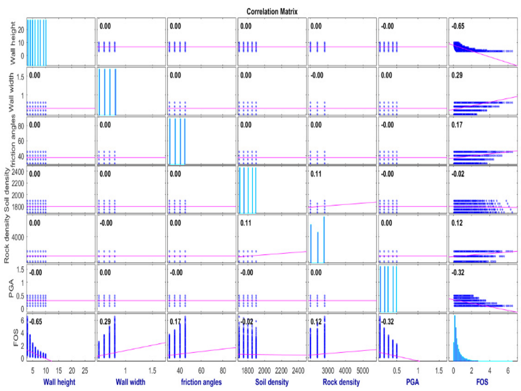

FIGURE 5. A matrix regression of all data.

TABLE 1. General description of applied data.

Parameter	Unit	Min	Average	Max
Wall height (H)	m	3	6.5	10
Wall width (B)	m	0.5	0.65	0.8
Internal friction angles	Degree	30	37.5	45
Soil density	Kg/m3	1700	1800	1900
Rock density	Kg/m3	2000	2426.67	2800
peak ground acceleration (PGA)	g	0.1	0.3	0.5
Factor of Safety (FOS)	-	0.027	0.568	6.476

to be 0.1, 0.2, 0.3, 0.4 and 0.5 g for horizontal direction and it was zero for vertical direction based on the scope of study. As noted before, the SF values can be calculated for different conditions, as 9600 models were simulated.

Table 1 provides a general description of various designs of a RW for dynamic conditions. The reason for these changes is engineering design to collect a strong dataset. Figure 5 shows the relationship between the parameters with each other as well as their distribution.

Finally, the flowchart designed for this research is presented in Figure 6. With this flowchart, a summary of the work to design the RWs engineering is provided.

III. RESULT AND DISCUSSION

A. ANN MODELING

It is generally accepted that ANN is a simulation method that designs simple to complex problems based on various functions. This system consists of various elements each of which performs its tasks together to improve the performance of models. The use of neural models to obtain appropriate models between parameters has increased the use of these methods. These methods can be called suitable alternatives to statistical methods such as multivariate regression and linear correlation.

In general, neural networks require methods that can teach them well [24], [25]. These methods, which are obtained by different algorithms, can change the system's performance. In the current study, the Multi-layer Perceptron (MLP), which consists of three layers, was used to predict the issue. Back-propagation (BP) algorithm is an algorithm that has been used by various researchers [26], [27]. These training algorithms include several layers that are most recommended using with three layers. Each layer contains nodes that have distinct classifications according to their locations. Nodes at the first layer are introduced as the input data. The second layer, which is also known as the hidden section of model, in fact contains neurons; and mathematical calculations can be used to find relationships between parameters. Finally, the output of this system is provided as an amount at the third layer.

In this research, based on recommendation of previous studies, a variety of neurons from 2 to 16 were tested for hidden layer. The number of neurons is one of the most important parameters affecting the results of the models. Outputs were evaluated according to coefficient of determination (R^2) and root mean square error (RMSE) results for comparing the efficiency of each training and testing datasets [28], [29]. As mentioned by previous researchers, the 80% of all data was assigned to the training part and the rest to the testing section. A selection comparison was made on the basis of a rating technique by Zorlu *et al.* [30]. In this technique, a score is assigned to each section. Similarly, the performance of the developed models was measured in terms of R^2 and RMSE for each system to compare. For example, R^2 values of 0.9863, 0.9864, 0.9865, 0.9865, 0.9944, 0.9934, 0.9941 and 0.9940 were achieved for models 1 to 8 of the training dataset with scores of 2, 3, 4, 4, 8, 5, 7, and 6 respectively. These scores were obtained for all row and then, their cumulative ranking was calculated in the last column. In this method, the score was created for 8 models; and the model with the highest score between others was considered as the best model. Table 2 presents results of the ANN model for predicting SF of RWs. As shown, model 5 with high precision of prediction, find the highest score and considered the selected model. A significant points of this table indicates that increasing the number of neurons at the hidden layer does not result in improved network performance due to the probability of occurrence in the ANN model. As the present study aimed to find the best ANN system and develop the network, the network was utilized to forecast SF in the RW. Figures 7 and 8, show results of implemented ANN in training as well as experimental steps for the model 5 (the best model). In these figures, measured and predicted values of SF are respectively obtained by the GeoStudio software and ANN.

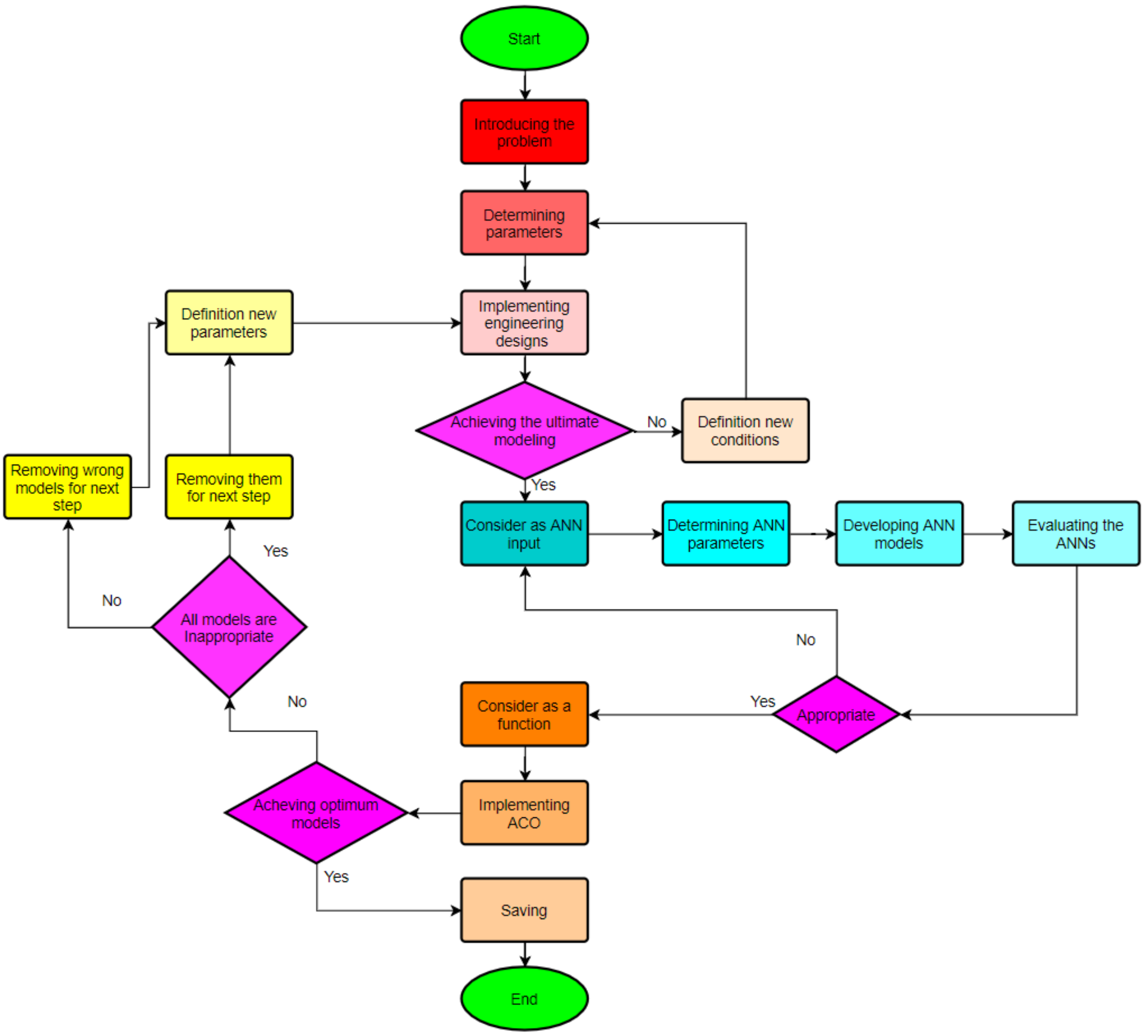

FIGURE 6. A general flowchart of the current study.

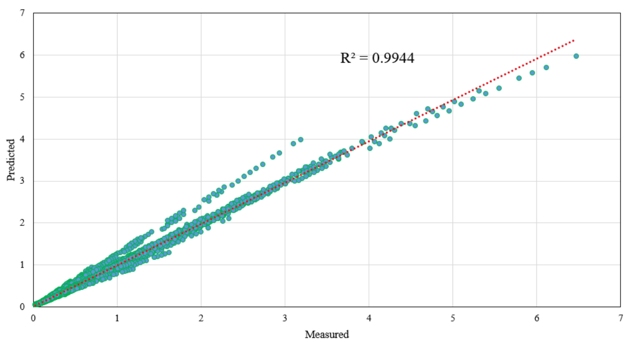

FIGURE 7. Training results for presented model 5 in Table.

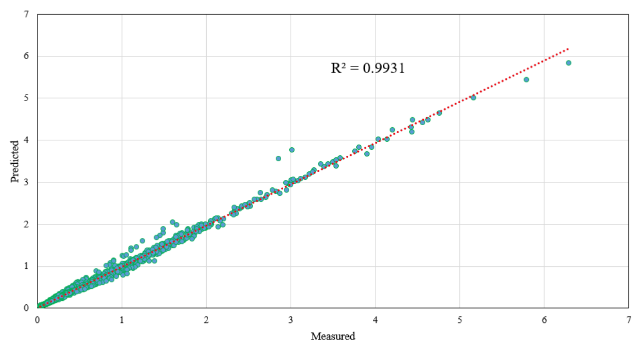

FIGURE 8. Testing results for presented model 5 in table 2.

High values of 0.9944 and 0.9931 for R^2 of training and testing steps respectively indicate the precision of the ANN model in forecasting the SF with the lowest error rate. In addition, results of the testing step of the model indicate that the network has a good ability to predict unknown data that can be considered as a validation. Results indicate the good modeling performance of the selected ANN in forecasting the SF of RWs in dynamic condition.

The ANN model selected as the best model was evaluated using different data. This will ensure that models are judged

TABLE 2. The results of designed models for predicting SF of RWs in dynamic conditions.

Model Number	Neuron No.	Train		Train		Train Rate		Test Rate		Total Rank
		R^2	RMSE	R^2	RMSE	R^2	RMSE	R^2	RMSE	
1	2	0.9863	0.1174	0.9848	0.1207	2	2	2	2	8
2	4	0.9864	0.1170	0.9849	0.1200	3	3	3	3	12
3	6	0.9865	0.1165	0.9851	0.1194	4	4	4	4	16
4	8	0.9865	0.1165	0.9824	0.1215	4	4	1	1	10
5	10	0.9944	0.0748	0.9931	0.0809	8	8	8	8	32
6	12	0.9934	0.0810	0.9919	0.0878	5	5	5	5	20
7	14	0.9941	0.0770	0.9924	0.0850	7	7	7	7	28
8	16	0.9940	0.0777	0.9923	0.0856	6	6	6	6	24

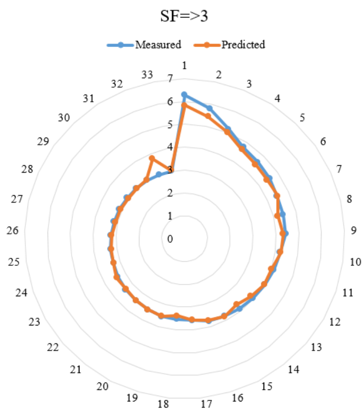

FIGURE 9. Predicted and measured values of new model for SF values greater than 3.

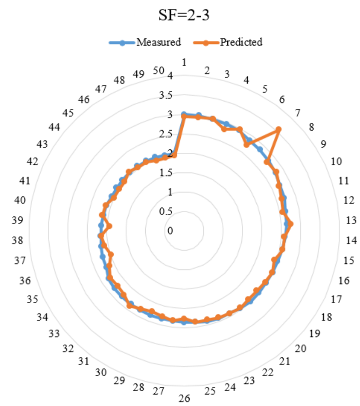

FIGURE 10. Predicted and measured values of new model for SF values between 2 and 3.

to be in a variety of situations. The amount of SF varies under different dynamic conditions. For various engineering design, three conditions were introduced to assess the ability of the new model. In Figures 9 to 11, evaluation results of three modes is shown. Figure 9 examines the model under conditions of a SF greater than 3. As it can be seen, the model can provide well-prediction in different conditions. Due to the importance of the SF, values for 2-3 and 1.5-2 are obtained in Figures 10 and 11, respectively. As a result, almost in all cases, the predicted SF values are close to measured values of SF. However, SF values greater than 3 are closer to measured SF values compared to SF = 2-3 and SF = 1.5-2.

B. DYNAMIC ANALYSIS OF RETAINING WALL STRUCTURE

In this research, an ACO algorithm for maximizing SF values of RWs was used. To this end, a model of cost function should be first provided. The model of cost function needs a proper relationship between input data and output. Here, the best model of ANN system was introduced as a function (model) to the ACO algorithm. It should be mentioned the all models were implemented in MATLAB environment. In this algorithm, various parameters and the constant values can effect on the ACO algorithm. The following description are considered in optimization modeling:

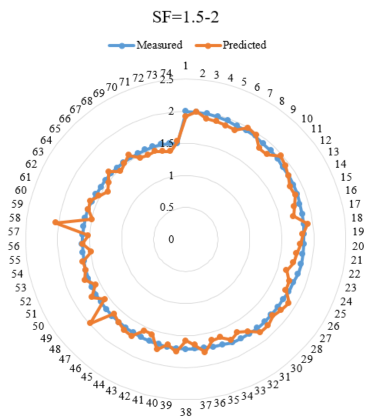

FIGURE 11. Predicted and measured values of new model for SF values between 1.5 and 2.

Q refers to constants for converting the minimum/ maximum function to the maximum/ minimum function.

α is introduced as critical parameter that can control or change the weights (pheromone)

β is a useful parameter for assigning weight to innovative information.

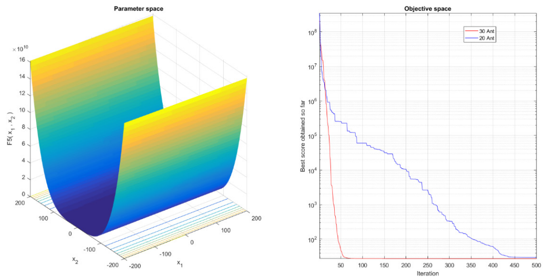

FIGURE 12. A comparison between 30 and 20 ants for the problem 1.

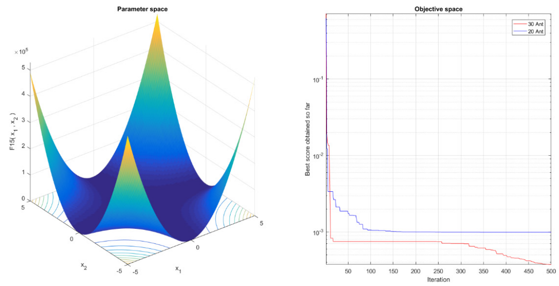

FIGURE 13. A comparison between 30 and 20 ants for the problem 2.

Repeat of a considered number for repetitions to find the optimal solution.

Ro: Assigned values to different ant routings.

The mentioned parameters are the main attributes of the ACO algorithm that can affect the performance of the optimization problem. The ''Ant routing'' program, which is assigned to find the shortest (best solution) routing, is according to a proper search that the ant chooses the shortest (best solution) route, and thus the defined function is improved (maximum). For implementation of this process, the first action should be done for producing 500 different part for the various solution in which the parts (routs) ware chosen randomly. In the following, the defined ants (populations) were forced to use different routes. It was found that there was an attitude to routes for ants from a particular route. A special route tends to find a higher values of pheromones than other routes. In the next step, the best range of routes were selected for each the data which introduced as input data (Table 1) by the ant routing algorithm indicating the minimum/ maximum cost function. The cost function is converted into the minimum/ maximum function by separating the defined function with a constant such as Q. After a while, the optimal route of each tour is obtained as the selected route. Thus, the action is repeated for whole remaining routes to find any other proper solution. A trial and error process was used to find ACO parameters. To determine the optimal values, two issues were considered separately. Then, with the number of 20 and 30 ants, the minimum values were obtained. Figures 12 and 13 show the results of this comparison. As it can be seen, the performance of 30 ant is better, as well as the number of iterations in two states of 500. For this reason, these two values were used to determine the conditions of the RWs engineering.

Figures 14-16 show the values of obtained results for maximizing the SF using this optimization algorithm. This process is used for each repeat to get the best response. As shown in the previous section, three designs were made to check the SF values more precisely. The SF values were 1.5-2, 2-3 and greater than 3 more detailed ones. Due to the importance of the amount of SF in different conditions, their optimal design can also be effective. For this reason, optimal designs were made to maximize the amount of SF for the stated conditions.

Figure 14 shows the optimization results for optimal design of the RWs in dynamic conditions and SF values higher

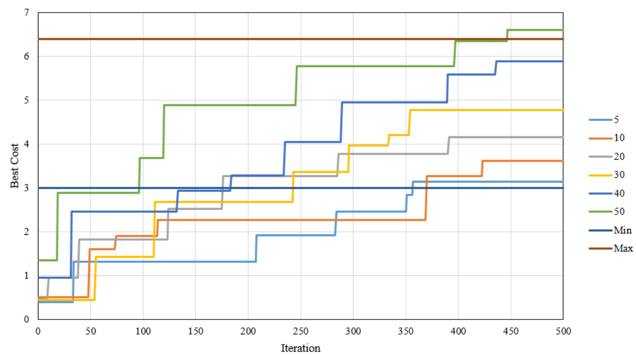

FIGURE 14. The result of ACO Algorithm for SF greater than 3.

TABLE 3. Optimization models built for SF greater than 3.

Number of Ant	Wall height (m)	Wall width (m)	Internal friction angles (degree)	Soil density (Kg/m3)	Soil density (Kg/m3)	PGA (g)	FS (-)
5	3	0.7	43.2	1722	2124.5	0.1	3.14
10	3.6	0.8	44.7	1723	2583.4	0.1	3.61
20	3.1	0.8	44.3	1816.5	2742	0.1	4.15
30	3.1	0.8	45	1863.7	2649.8	0.1	4.78
40	3	0.7	42.8	1806.5	2712.8	0.1	5.89
50	3	0.8	44.9	1720	2780	0.1	6.61

than 3. The parameters used in this study were designed to implement RWs with SF values of between 3 and 6.4. To evaluate the effect of different parameters of the ACO algorithm, the number of iteration in all designs was 500. Then, the effect of ant number on obtaining optimal conditions was evaluated.

As it can be seen in Figure 14, all results of SF values provide the higher values than the lowest (3). By increasing the number of ant, the optimal values of RWs will increase. One of the reasons for this increase is due to the impact of a population that can better identify optimal conditions. This makes it possible to reduce the engineering error in different conditions and increase the design performance. In addition, the amount of ant = 50 is able to provide a better condition than the maximum value for a SF in dynamic conditions. Finally, the optimal parameters were obtained for each mode. These parameters are given in Table 3. With these parameters, the performance of RWs can be improved.

For the latter, the same processes of the first state were repeated. The minimum and maximum values for this state

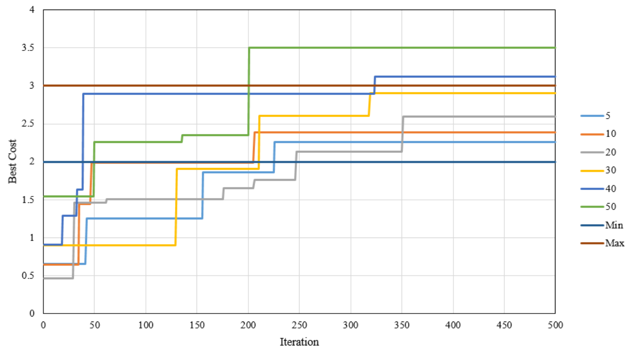

FIGURE 15. The result of ACO Algorithm for SF = 2-3.

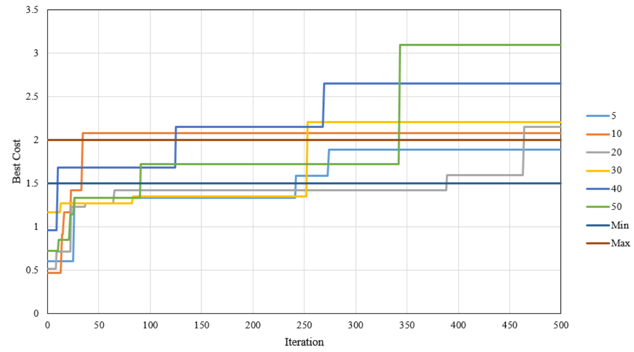

FIGURE 16. The result of ACO algorithm for SF = 1.5-2.

TABLE 4. Optimization models built for SF = 2-3.

Number of Ant	Wall height (m)	Wall width (m)	Internal friction angles (degree)	Soil density (Kg/m3)	Soil density (Kg/m3)	PGA (g)	FS (-)
5	4	0.7	43.9	1717.9	2624.2	0.1	2.25
10	3.3	0.8	41.4	1778.6	2291.1	0.1	2.38
20	3.3	0.6	39.4	1722.6	2729.7	0.1	2.59
30	3	0.7	42.2	1866.2	2106.4	0.1	2.90
40	3	0.8	43.3	1812.5	2271.5	0.1	3.12
50	3	0.5	45	1900	2800	0.1	3.50

TABLE 5. Optimization models built for SF = 1.5-2.

Number of Ant	Wall height (m)	Wall width (m)	Internal friction angles (degree)	Soil density (Kg/m3)	Soil density (Kg/m3)	PGA (g)	FS (-)
5	3.3	0.8	44.4	1729.5	2306	0.3	1.89
10	3.4	0.7	39	1824.7	2480.5	0.2	2.08
20	3	0.5	38.4	1700	2000	0.2	2.15
30	3.1	0.8	38.1	1730.3	2625.6	0.3	2.20
40	3	0.8	43.3	1707	2271.5	0.1	2.65
50	3.4	0.7	44.6	1707	2770.5	0.2	3.09

are between 2-3. As shown in Figure 15, all surveys are better than the minimum amount of SF. In addition, with two ant values of 40 and 50, it also offers better performance. With these conditions, the precision in the design of the RWs is increased in dynamic conditions. Table 4 provides optimal values for this mode.

One of the important parts in engineering design is to increase SF values (mostly greater than 1). In most designs, the SF value is about 1.5-2. Therefore, the conditions for this interval were examined by ACO optimization algorithm. The previous steps are implemented here. However, ant values above 5 showed a better performance than baseline conditions. These results show that if the range of variations is lower, better performance can be obtained for optimal conditions. The results of this section are shown in Figure 16. Finally, the optimal values for these conditions are given in Table 5 for the RWs. All of above procedures can be done in different situations and intervals for designing engineering of RWs.

IV. CONCLUSION

In the present study, a hybrid model of ANN and ACO was implemented to forecast and optimize RWs under dynamic conditions. The applied data was obtained by coding more than 9000 different states. Various data was used with effects on dynamics of RW structure. After trial and error process, an ANN model was proposed based on training algorithm of LM with combination of 6-10-1 to forecast the SF values of RWs. This network was properly selected by scoring method. The best ANN model was used as an input of ACO for optimization purposes. The ACO algorithm evaluated the wall under dynamic conditions using various factors. Different and effective parameters for increasing SF values were identified, and optimal states were designed. The states indicated that effects of parameters should be carefully evaluated in dynamic conditions. This could control potential problems during dynamic loads.

REFERENCES

[1] N. Mononobe, "On determination of earth pressure during earthquake," in *Proc. World Eng. Congr.*, 1929, pp. 177–185.
[2] S. Okabe, "General theory of earth pressure," *J. Jpn. Soc. Civil Eng.*, vol. 12, no. 1, 1926.
[3] G. Mylonakis, P. Kloukinas, and C. Papantonopoulos, "An alternative to the Mononobe–Okabe equations for seismic earth pressures," *Soil Dyn. Earthq. Eng.*, vol. 27, no. 10, pp. 957–969, 2007.
[4] S. Nakamura, "Reexamination of Mononobe–Okabe theory of gravity retaining walls using centrifuge model tests," *Soils Found*, vol. 46, no. 2, pp. 135–146, 2006.
[5] L. Al Atik and N. Sitar, "Experimental and analytical study of the seismic performance of retaining structures," *Pacific Earthq. Eng. Res. Center*, to be published.
[6] M. M. Dewoolkar, H.-Y. Ko, and R. Y. S. Pak, "Seismic behavior of cantilever retaining walls with liquefiable backfills," *J. Geotech. Geoenviron. Eng.*, vol. 127, pp. 424–435, May 2001.

[7] R. A. Green and R. M. Ebeling, "Seismic analysis of cantilever retaining walls, Phase I," Earthq. Eng. Res. Program, U.S. Army Corps Eng., Washington, DC, USA, 2002.
[8] G. Gazetas, P. N. Psarropoulos, I. Anastasopoulos, and N. Gerolymos, "Seismic behaviour of flexible retaining systems subjected to short-duration moderately strong excitation," *Soil Dyn. Earthq. Eng.*, vol. 24, no. 7, pp. 537–550, 2004.
[9] P. N. Psarropoulos, G. Klonaris, and G. Gazetas, "Seismic earth pressures on rigid and flexible retaining walls," *Soil Dyn. Earthq. Eng.*, vol. 25, pp. 795–809, Aug./Oct. 2005.
[10] F. Ostadan, "Seismic soil pressure for building walls: An updated approach," *Soil Dyn. Earthq. Eng.*, vol. 25, pp. 785–793, Aug./Oct. 2005.
[11] J. Wood, "Earthquake-induced soil pressures on structures," Earthq. Eng. Res. Lab., California Inst. Technol., Pasadena, CA, USA, Tech. Rep. EERL 73-05 1973.
[12] M. Kong and P. Tian, "Application of ACO in continuous domain," in *Proc. Int. Conf. Natural Comput.*, 2006, pp. 126–135.
[13] M. Koopialipoor, B. R. Murlidhar, A. Hedayat, D. J. Armaghani, B. Gordan, and E. T. Mohamad, "The use of new intelligent techniques in designing retaining walls," *Eng. Comput.*, pp. 1–12, Jan. 2019. doi: 10.1007/s00366-018-00700-1.
[14] S. Mazzeo and I. Loiseau, "An ant colony algorithm for the capacitated vehicle routing," *Electron. Notes Discrete Math.*, vol. 18, pp. 181–186, Dec. 2004.
[15] X. Liao, M. Khandelwal, H. Yang, M. Koopialipoor, and B. R. Murlidhar, "Effects of a proper feature selection on prediction and optimization of drilling rate using intelligent techniques," *Eng. Comput.*, pp. 1–12, Jan. 2019. doi: 10.1007/s00366-019-00711-6.
[16] M. Koopialipoor, D. J. Armaghani, A. Hedayat, A. Marto, and B. Gordan, "Applying various hybrid intelligent systems to evaluate and predict slope stability under static and dynamic conditions," *Soft Comput.*, vol. 23, no. 14, pp. 5913–5929, 2018.
[17] E. N. Ghaleini, M. Koopialipoor, M. Momenzadeh, M. E. Sarafraz, E. T. Mohamad, and B. Gordan, "A combination of artificial bee colony and neural network for approximating the safety factor of retaining walls," *Eng. Comput.*, vol. 35, no. 2, pp. 647–658, 2018.
[18] M. Koopialipoor, A. Fahimifar, E. N. Ghaleini, M. Momenzadeh, and D. J. Armaghani, "Development of a new hybrid ANN for solving a geotechnical problem related to tunnel boring machine performance," *Eng. Comput.*, pp. 1–13, Jan. 2019.
[19] Y. Zhao, A. Noorbakhsh, M. Koopialipoor, A. Azizi, and M. M. Tahir, "A new methodology for optimization and prediction of rate of penetration during drilling operations," *Eng. Comput.*, pp. 1–9, Jan. 2019. doi: 10.1007/s00366-019-00715-2.
[20] M. Koopialipoor, E. N. Ghaleini, M. Haghighi, S. Kanagarajan, P. Maarefvand, and E. T. Mohamad, "Overbreak prediction and optimization in tunnel using neural network and bee colony techniques," *Eng. Comput.*, pp. 1–12, Oct. 2018.
[21] M. Dorigo, V. Maniezzo, and A. Colorni, "Ant system: Optimization by a colony of cooperating agents," *IEEE Trans. Syst., Man, Cybern. B, Cybern.*, vol. 26, no. 1, pp. 29–41, Feb. 1996.
[22] H. R. Maier, A. R. Simpson, A. C. Zecchin, W. K. Foong, K. Y. Phang, H. Y. Seah, and C. L. Tan, "Ant colony optimization for design of water distribution systems," *J. Water Resour. Planning Manage.*, vol. 129, pp. 200–209, May 2003.
[23] C. Zecchin, H. R. Maier, A. R. Simpson, M. Leonard, and J. B. Nixon, "Ant colony optimization applied to water distribution system design: Comparative study of five algorithms," *J. Water Resour. Planning Manage.*, vol. 133, no. 1, pp. 87–92, Jan. 2007.
[24] M. Koopialipoor, E. N. Ghaleini, H. Tootoonchi, D. J. Armaghani, M. Haghighi, and A. Hedayat, "Developing a new intelligent technique to predict overbreak in tunnels using an artificial bee colony-based ANN," *Environ. Earth Sci.*, vol. 78, p. 165, Feb. 2019. doi: 10.1007/s12665-019-8163-x.
[25] M. Koopialipoor, A. Fallah, D. J. Armaghani, A. Azizi, and E. T. Mohamad, "Three hybrid intelligent models in estimating flyrock distance resulting from blasting," *Eng. Comput.*, vol. 35, no. 1, pp. 243–256, 2018.
[26] M. Hasanipanah, D. J. Armaghani, H. B. Amnieh, M. Koopialipoor, and H. Arab, "A risk-based technique to analyze flyrock results through rock engineering system," *Geotech. Geolog. Eng.*, vol. 36, no. 4, pp. 2247–2260, 2018.
[27] M. Koopialipoor, D. J. Armaghani, M. Haghighi, and E. N. Ghaleini, "A neuro-genetic predictive model to approximate overbreak induced by drilling and blasting operation in tunnels," *Bull. Eng. Geol. Environ.*, vol. 78, no. 2, pp. 981–990, 2017.
[28] M. Koopialipoor, S. S. Nikouei, A. Marto, A. Fahimifar, D. J. Armaghani, and E. T. Mohamad, "Predicting tunnel boring machine performance through a new model based on the group method of data handling," *Bull. Eng. Geol. Environ.*, vol. 78, no. 5, pp. 3799–3813, 2018.
[29] J. Zhou, N. Aghili, E. N. Ghaleini, D. T. Bui, M. M. Tahir, and M. Koopialipoor, "A Monte Carlo simulation approach for effective assessment of flyrock based on intelligent system of neural network," *Eng. Comput.*, pp. 1–11, Mar. 2019. doi: 10.1007/s00366-019-00726-z.
[30] K. Zorlu, C. Gokceoglu, F. Ocakoglu, H. A. Nefeslioglu, and S. Acikalin, "Prediction of uniaxial compressive strength of sandstones using petrography-based models," *Eng. Geol.*, vol. 96, pp. 141–158, Feb. 2008.